Annual to Daily Ice Velocity and Water Pressure Variations on Ka Roimata o Hine Hukatere (Franz Josef Glacier), New Zealand

Authors: Anderson, Brian, Willis, Ian, Goodsell, Becky, Banwell, Alison, Owens, Ian, et al.

Source: Arctic, Antarctic, and Alpine Research, 46(4) : 919-932

Published By: Institute of Arctic and Alpine Research (INSTAAR), University of Colorado

URL: https://doi.org/10.1657/1938-4246-46.4.919

Arctic, Antarctic, and Alpine Research, Vol. 46, No. 4, 2014, pp. 919–932

Annual to daily ice velocity and water pressure variations on Ka Roimata o Hine Hukatere (Franz Josef Glacier), New Zealand

Brian Anderson§*
Ian Willis†
*Becky Goodsell**
Alison Banwell†
Ian Owens‡
Andrew Mackintosh and*
Wendy Lawson‡

*Antarctic Research Centre, Victoria University, PO Box 600, Wellington, New Zealand
†Scott Polar Research Institute, Department of Geography, University of Cambridge, Lensfield Road, Cambridge CB2 1ER, UK
‡Department of Geography, University of Canterbury, Private Bag 4800, Christchurch, New Zealand
§Corresponding author: brian.anderson@vuw.ac.nz

Abstract

Ka Roimata o Hine Hukatere (Franz Josef Glacier) is a fast-flowing maritime glacier and its climatological and hydrological drivers are different from those of many previously studied alpine glaciers. The glacier tongue has recently advanced as well as retreated, remains largely snow free, has significant volumes of melt and rainwater inputs throughout the year, and experiences small radiation and air temperature fluctuations over diurnal to seasonal time scales. We discuss measurements of surface velocity made between 2000 and 2012 at annual, seasonal, weekly, and daily time scales together with measurements of glacier geometry change, and calculations of surface water inputs and subglacial water pressure variations derived from a distributed surface mass balance model and a one-dimensional conduit hydrology model, respectively. Annual velocity variations are linked to changes in glacier geometry and advance/retreat cycles with accelerations during thickening and advance and decelerations during thinning and retreat. At seasonal, weekly and daily time scales, velocities are correlated with water input variations and with rates of water pressure fluctuation rather than absolute magnitudes of water pressure.

DOI: http://dx.doi.org/10.1657/1938-4246-46.4.919

Introduction

Over long time scales (years to decades), glacier velocities adjust to the overall stress regime influenced by changes in glacier geometry, notably thickness and slope. Over shorter time scales (weeks, months, and seasons), velocities respond sensitively to shorter term variations in the stress patterns brought about by changes in the quantity and pressure of water at the glacier bed. Compared to glaciers in Europe and North America, there have been very few studies of glacier velocity variations in the Southern Alps of New Zealand, although notable exceptions include Gunn (1964), McSaveney and Gage (1968), and Purdie et al. (2008). There are reasons to expect that variations in ice velocity of New Zealand glaciers at a variety of time scales might be different from those of glaciers in Europe and North America.

First, over the past few years to decades the climate forcing of the highly maritime New Zealand glaciers has been different from that of many glaciers elsewhere, especially those in continental settings. Most European and North American glaciers have been responding to net warming since the 1980s, to lower accumulation and higher ablation rates compared to the 1970s, and have undergone almost continuous retreat (Leclercq and Oerlemans, 2011). Glacier changes in the Southern Alps have been more complicated, where glaciers with higher mass turnover and short response times, such as Ka Roimata o Hine Hukatere or Franz Josef Glacier (FJG), have undergone several advance/retreat cycles. This behavior provides an opportunity to examine the relationships between geometry and velocity during recent advance as well as retreat stages at FJG. The large and rapid changes in ice thickness and surface slope associated with advance and retreat over the past decade suggest that there will also be large and systematic variations in ice velocity. Previous work has suggested that ice velocity increases tend to be linked to periods of positive mass balance leading to increases in ice thickness, possibly surface gradients, and therefore driving stresses (Span et al., 1997; Vincent et al., 2009; Herman et al., 2011).

Second, over weeks, months, and seasons, the climate and hydrological forcing of New Zealand glaciers has also likely been different from that of many glaciers elsewhere, especially those in continental regions. Continental glaciers have high amplitude seasonal cycles of radiation and temperature, with temperatures dropping to well below freezing in the winter. This results in marked seasonality in water inputs to the glacier bed, as during winter there is little or no melt, and most precipitation falls as snow (Willis, 1995). In the maritime Southern Alps of New Zealand, the seasonal variations in radiation and temperature are much smaller, with temperatures, especially at low elevations, remaining above freezing for much of the time, even in winter (Anderson and Mackintosh, 2012). Furthermore, many of the glaciers receive very high rates of precipitation—up to ~10 m a^{-1} at FJG (Griffiths and McSaveney, 1983). Consequently, there can be high rainfall and ablation events in winter with only a moderate seasonality in water inputs to the glacier bed. For example, Owens et al. (1984) reported a rainfall event in June 1981 where >0.3 m of rain fell in 19 hours with a resulting ablation rate of ~0.2 m water equivalent (w.e.) per day.

Additionally, since many of the long, steep glaciers in the Southern Alps extend to low elevations, their tongues remain largely snow free, even in the winter. Furthermore, the surface energy balance is dominated less by shortwave radiation fluxes and more by turbulent fluxes compared to continental glaciers (Ishikawa et al., 1992; Willis et al., 2002, their Table III; Anderson et al., 2010).

Consequently, weekly variations in velocity measured over a few months, and daily variations recorded over a few weeks, might be expected to be smaller than at continental glaciers. Melt and rain inputs throughout the winter might allow a channelized drainage system to survive the winter, reducing the likelihood of the "spring-event." The "spring event" is defined as glacier uplift and acceleration lasting a few days associated with rapid increases in subglacial water pressures when a predominantly distributed drainage system is overwhelmed by the sudden increase in meltwater to the bed associated with the depletion of the winter snowpack (Iken et al., 1983; Mair et al., 2003). Throughout the summer, daily velocity variations might also be expected to be less marked than at continental glaciers since meltwater inputs will be less variable, although velocities might be expected to increase in response to heavy rainstorms.

Aims and Methodology

Measurements of ice velocity have been made on the lower part of FJG over a variety of time intervals at a variety of resolutions between 2000 and 2012. We have split the measurements to examine the extent of velocity variations and their causes over four time scales: (1) annual variations measured over 12 years, (2) seasonal variations measured over 2 years, (3) weekly variations measured over five months, (4) daily variations measured over two weeks. Based on these observations, we aim to test four related hypotheses:

1. The distinctive pattern of recent climate change over the Southern Alps, resulting in glacier advance as well as retreat, will have caused greater annual variability in velocity at FJG compared to many glaciers elsewhere, which have simply undergone terminus retreat and slowdown.
2. Because the glacier tongue is thin and steep and remains largely snow-free in the winter, and because of the year-round abundance of meltwater and rainwater, a channelized subglacial drainage system will dominate throughout the year, and seasonal variations in subglacial water pressure and therefore glacier velocity will be more limited on FJG compared to elsewhere.
3. "Spring events," where rapidly increasing water inputs to a hydraulically inefficient subglacial drainage system cause large velocity increases, will not occur at FJG because a channelized subglacial drainage system will not close down over the winter, will dominate throughout the year, and will be able to accommodate the relatively small increases in surface meltwater in the spring.
4. The limited daily radiation and temperature range and variability over glaciers in the Southern Alps will result in smaller daily velocity variations on FJG compared to many glaciers elsewhere.

Our overall methodology is to compare measured ice velocity variations at the four time scales mentioned above with the expected controlling variables. In the case of the annual changes, we expect ice thickness and surface gradient to be key controls; thus, we show how the geometry and terminus position have changed between 2000 and 2012 in order to help interpret the annual variations in velocity. In the case of the seasonal, weekly, and daily velocity variations, we expect the controls to be water pressure variations across the glacier bed driven by water inputs to the glacier (melt and rainfall) and the capacity of the drainage system to accommodate them. To help interpret the velocity variations over these time scales, we use a spatially distributed modeling approach to calculate patterns of meltwater and rainwater inputs across the glacier surface, and a one-dimensional hydrological model to route this water beneath the glacier. Key outputs we use from the models are temporal patterns of bulk (glacierwide) water inputs to the glacier and spatial and temporal patterns of water pressure along the glacier length, enabling us to identify links between these and patterns of measured surface velocity at the seasonal to daily time scales.

Study Area

FJG is a temperate maritime glacier situated on the western side of New Zealand's Southern Alps (43°29′S, 170°11′E) (Fig. 1) with an area of ~36 km^2 in 2000. The topographic and climatic conditions of the area include high relief, steep slopes, and high precipitation rates, resulting in glaciers with high mass turnovers that are very fast-flowing, typically up to 5 m d^{-1} (Fig. 1; Herman et al., 2011). FJG is approximately 11 km long, consisting of a relatively large (~28 km^2) accumulation basin between the altitudes of ~1800 and 2900 m, and a tongue that descends from ~1800 to ~300 m. A mean annual temperature of 11.1 °C (1970–2000) was measured at Franz Josef village, 7 km to the north at 155 m a.s.l. (New Zealand climate database, http://cliflo.niwa.co.nz). The glacier receives high annual precipitation (e.g., ~10 m a^{-1} measured adjacent to the glacier tongue, reported by Griffiths and McSaveney, 1983), and large precipitation events can occur at any time of year. The upper basin receives up to 8 m w.e. a^{-1} of accumulation (Anderson et al., 2006). On the glacier tongue, snowfall is rare and there is year-round ablation totaling up to ~20 m w.e. a^{-1} (Anderson et al., 2006). The glacier has one of the longest and most detailed records of terminus position in the Southern Hemisphere (Grove, 2004) and has been through a retreat-advance-retreat cycle during our period of field data collection, 2000–2012. The relative ease of year-round access to FJG has enabled the collection of velocity measurements over a variety of time scales.

Methods

SURFACE VELOCITY

All velocities presented here are calculated from the horizontal displacement of markers on the glacier between two time intervals, measured by repeat surveys to a network of stiff PVC stakes drilled into the glacier surface.

Annual, seasonal, and weekly velocities were measured by repeat differential GPS surveys using Trimble 4700 receivers. The GPS data were processed using Trimble Software using base data from a station 2 km from the glacier terminus (Fig. 1), which typically resulted in reported horizontal errors in the range 0.01 to 0.02 m. The typical total horizontal root-mean-square error (RMSE) in stake positioning is calculated to be 0.12 m, which is made up of the GPS error of 0.02 m, antenna positioning error of 0.06 m, and an error arising from stakes not being perfectly vertical of 0.10 m. Annual and seasonal velocities were also measured with a Trimble GeoXH receiver differentially corrected against base data at most 100 km away resulting in higher errors totaling approximately 1 m. In each velocity plot, the errors for each measurement are shown as error bars. When each stake had moved more than 50 m, it was relocated to its original site. This approach was needed because of the limited number of safe areas available for stakes and their rapid movement into crevassed areas.

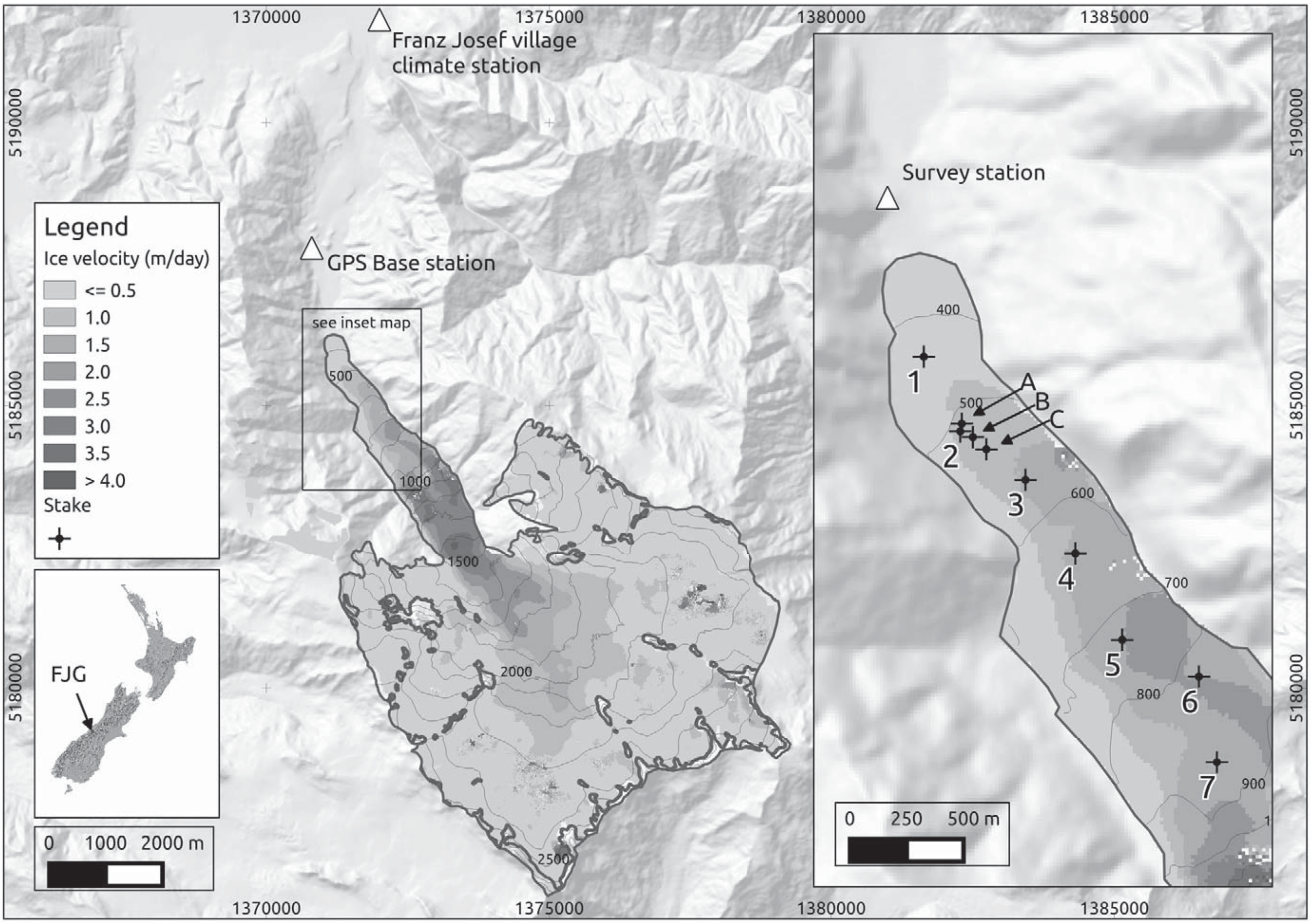

FIGURE 1. Location map of Franz Josef Glacier (FJG) indicating stake positions. The glacier outline is obtained from 2009 ASTER satellite imagery (GLIMS and NSIDC, 2005) and is shaded according to velocity (m d^{-1}) observed 29 January to 14 February 2002 (Herman et al., 2011). Daily velocities are derived from measurements made to stakes A, B, and C, weekly velocities are obtained from surveys to stakes 2, 3, 5, 6, and 7, and seasonal and annual velocities are produced for stakes 2 and 3. The map also shows the survey station used for the daily surveys, the GPS base station used for the weekly surveys, and Franz Josef village, where long-term meteorological measurements are available. Contours are shown at 100 m elevation spacing. The map uses the NZTM projection.

Daily measurements were made from surveys to a network of stake-mounted prisms using a Leica Total Station (Fig. 1). The survey station was located on bedrock at Champness Rock, ~500 m from the glacier snout, at an elevation of 300 m, at approximately the same elevation as the glacier stakes, which moved toward the station. Since errors associated with measuring angles are typically greater than those associated with determining distance, the position of the survey station ensured errors were kept to a minimum. Individual survey errors of ±0.02 m were measured, giving RMSEs ±0.03 m d^{-1} for daily velocities. Stakes remained in the same positions for these short-term surveys, and were kept vertical in their holes by redrilling the same hole deeper and/or by the addition of wedges as the holes ablated.

SURFACE ELEVATION

A 100 m digital elevation model (DEM) of the glacier surface and surrounding topography at the start of the glacier velocity measurement period (2000) was obtained from the Shuttle Radar Topography Mission (SRTM) product. The glacier surface long profile is shown in Figure 2.

Between 2000 and 2012, surface elevation data were collected along the approximate centerline of the glacier snout using a backpack-mounted GPS receiver, which was a Trimble 4700, GeoXH, or ProXL system. Surveys reported here were made annually, generally during early winter (April/May), and were postprocessed using various base station data sets with baselines from 2 km (using the base station in Fig. 1) to 200 km (using a permanent GPS station in Christchurch). The postprocessed data were averaged every 20 to 30 data points, to give a surface elevation measurement every 50 m along the glacier centerline. To compare the surface elevation data from year to year, the GPS positions were converted to a distance from the fixed survey station position on Champness Rock in front of the glacier terminus (Fig. 1). The GPS vertical error is as high as ~6 m, due largely to the long baseline between the glacier and base station. Furthermore, the precise location of the profile varied slightly each year depending on safe access to and on the glacier, although it was kept as central and consistent between years as possible. As we take the profiles to represent the glacier elevation along an approximate centerline, the vertical error is estimated by taking the distance of each measured elevation

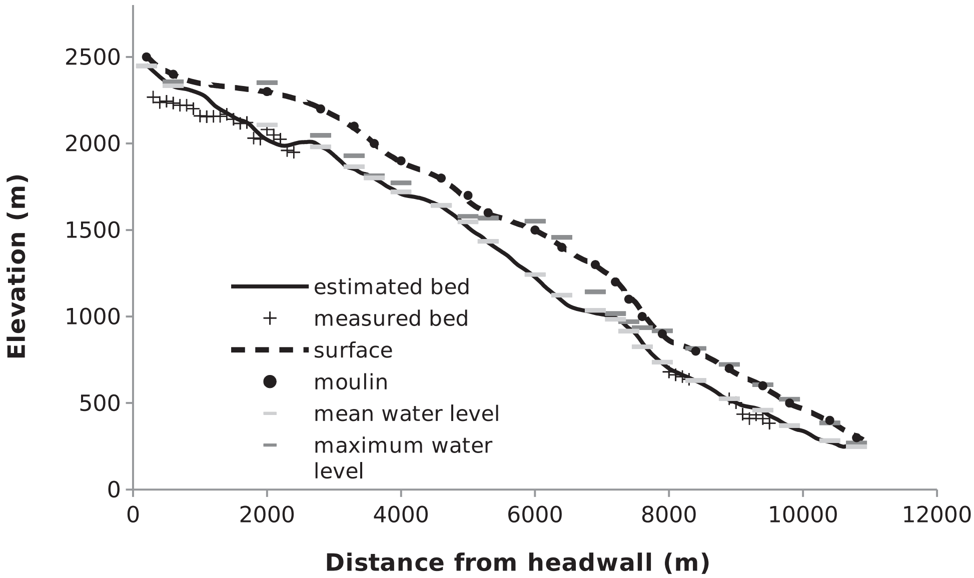

FIGURE 2. Surface and bed profiles along the glacier centre line. The surface profile is derived from Shuttle Radar Topography Mission data. The estimated bed profile is derived by the mass-flux method as described in the text, which is constrained by the measured bed elevations. The locations of the moulins used in the hydrological model are also the positions of the 100 m surface elevation contours. The mean and maximum subglacial water pressures (expressed as moulin water levels) calculated by the hydrological model between 01 November 2003 and 28 March 2004 are also shown.

from the glacier centerline, and a nominal cross-glacier gradient of 0.1, estimated from observed topographic variability on the glacier. This results in error estimates that vary from ~1 m (using the local base station and surveying close to the centerline) to ~15 m (using the remote base data and surveying further from the centerline). Despite this, the measured elevation change between years is often of the order of several tens of metres and so we are confident that the surveys provide a useful indication of the surface height change along the glacier snout. The error range of each measurement is plotted on the time series and glacier profiles.

BED ELEVATION

An estimate of the bed elevation along the centerline was obtained by subtracting calculated ice thickness estimates from the 2000 surface DEM, which is the most recent complete DEM of the glacier (Fig. 2). Ice thickness data were calculated based on the method described by Farinotti et al. (2009). It uses the principle of mass conservation—that is, that the mass balance distribution should be balanced by the ice flow and any surface elevation change. We use the output from a surface mass balance model (Anderson and Mackintosh, 2012) run for the years 2000–2010 across the surface DEM (Fig. 3) to calculate ice-flux divergence across the glacier. As there is insufficient information on surface elevation changes at FJG, we assume that the surface elevation in 2000 is in equilibrium with the mean 2000–2010 mass balance, based on the near-zero (–0.11 m w.e.) area-averaged mass balance over the period. Because we are mainly interested in the lower glacier, we simplify the Farinotti et al. (2009) method, and rather than delineating "ice flow catchments" for specific ice flow-lines, the total integrated up-glacier mass flux is used, and distributed across elevation bands depending on the distance from the glacier margin. The ice thickness is then calculated from equation 7 of Farinotti et al. (2009) from the ice-flux and three flow parameters. Using a standard value of the flow rate factor $A = 6.8 \times 10^{-15}$ s^{-1} kPa^{-3}, and the flow exponent $n = 3$, the flow correction factor C in equation 7 of Farinotti et al. (2009) is then adjusted to minimize the RMSE between calculated ice thickness and measured ice thickness along the centerline at the 22 locations in the upper basin and 11 places on the lower tongue where the bed topography is known from radio-echo sounding (Anderson et al., 2008) (Fig. 2). The resulting value of the correction factor is $C = 1.3$. The RMSE between measured ice thickness at the 33 locations where we have measurements and ice thickness calculated using the mass flux method is 64 m (32% of the mean depth at measured locations).

MODELED WATER INPUTS

Water inputs to the glacier were calculated using the spatially distributed surface mass balance model described by Anderson and Mackintosh (2012). For each day of each glacier year for the decade 2000–2010 (1 April 2000 to 31 March 2011), the mass balance model was driven using meteorological data provided by the National Institute of Water and Atmospheric Research's Virtual Climate Station Network (VCSN), an interpolation of climate station data using a trivariate spline on a 0.05° resolution grid (Tait and Turner, 2005). The grid square with Franz Josef village close to its center was used. Key model parameter values have been optimized using data from FJG and other nearby glaciers (Anderson and Mackintosh, 2012) and are given in Table 1. The key model output relevant to this study is spatially and temporally varying surface water inputs from melt and rain.

MODELED SUBGLACIAL WATER PRESSURES

The hydrological model used to calculate subglacial water pressures is derived from the Extended Transport (EXTRAN) block of the United States Environmental Protection Agency's (EPA) Storm Water Management Model (SWMM) (Roesner et al., 1988) and has previously been applied successfully to both Haut Glacier d'Arolla, Switzerland (Arnold et al., 1998), and the Paakitsoq region of the Greenland Ice Sheet (Banwell et al., 2013). The hydrological model uses the one-dimensional St. Venant momentum and continuity equations (i.e., the shallow-water equations) to route the water through channel segments. The code has been adapted (Arnold et al., 1998) to enable the diameter of each channel segment to enlarge through wall melting and shrink by creep closure at each model time-step (after Spring and Hutter, 1981).

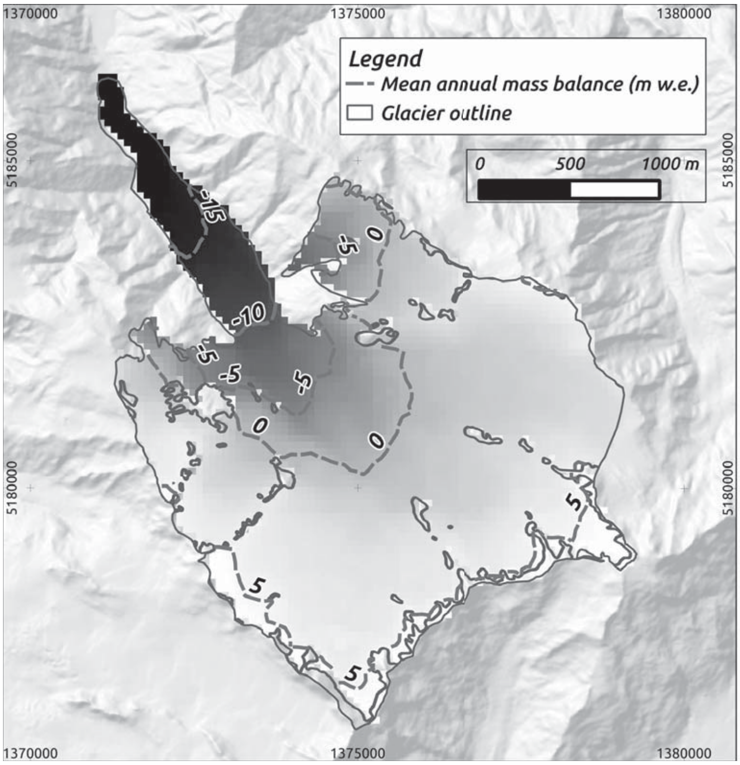

FIGURE 3. Mean annual mass balance over the 2000/2001 to 2010/2011 period as estimated by the energy balance model.

TABLE 1

Parameter values used in the surface mass balance and hydrology models.

Parameter	Parameter value
Mass balance model	
Snow albedo	0.90
Ice albedo	0.36
Temperature lapse rate	0.005 °C m^{-1}
Threshold temperature for rain/snow	1 °C
Hydrology model	
Fixed junction area	1 m^2
Initial channel diameter	1 m
Minimum channel diameter	0.01 m
Manning roughness	0.07 s $m^{-1/3}$
Rate factor in ice flow law	6.8×10^{-15} s^{-1} kPa^{-3}
Exponent in ice flow law	3

Time-dependent outputs from the model are channel cross-sectional areas, and water velocities, discharges, and pressures. Further details of the model can be found in Roesner et al. (1988), Arnold et al. (1998), and Banwell et al. (2013).

The model's subglacial drainage system is inherently "channelized"; a "distributed" drainage system and the interaction of the channelized system with a distributed system are not explicitly accounted for. However, as mentioned above, FJG tongue is relatively thin and steep, it remains largely snow free throughout the year, and it receives high rates of meltwater and rainwater inputs throughout the year, even in winter. For these reasons, we hypothesize that a channelized subglacial drainage system exists and dominates throughout the year. We explore the validity of this assumption by comparing model outputs, notably subglacial water pressure variations, with those we would infer from the glacier velocity measurements.

We do not have enough data from FJG to parameterize the surface routing algorithms across snow and ice used by Arnold et al. (1998) and Banwell et al. (2012, 2013). Nor do we have an accurate enough representation of the distribution of moulins across the glacier to model precisely the delivery of water to the glacier bed, as these previous authors did. Finally, we do not have an accurate enough bed DEM to allow us to prescribe the location of the main hydrological pathways across the bed of the glacier as was done for Haut Glacier d'Arolla, Switzerland (Arnold et al., 1998) and part of the Greenland Ice Sheet (Banwell et al., 2013). We therefore take a more idealized approach to the routing of water across the glacier surface and bed, and to the calculation of subglacial water pressures. We simplify the problem to one dimension and assume a subglacial circular channel runs along the length of the glacier centerline. The glacier is divided into 100-m horizontal sections and subglacial channel segments are designated for each section. The model is insensitive to the precise value used for the length of each section. The bed elevations at the upper and lower end of each channel segment are prescribed from the bed profile. The segments are joined by junctions, which are represented in the model as vertical circular shafts extending from the glacier bed to the surface. The diameter of all junctions is fixed and prescribed. The initial diameter of each channel segment can vary and is prescribed, as is the minimum diameter that each segment can attain. The key parameter values used in the model are shown in Table 1. Although the absolute magnitudes of model outputs depend on the precise values of some of the parameters used, the spatial and temporal patterns of model outputs (which we are interested in here) are insensitive to these (Arnold et al., 1998). Junctions that lie closest to the locations of the 100 m surface elevation contours are designated as moulins, and can receive surface meltwater inputs. For each 100 m surface elevation band, the melt and rain calculated by the mass balance model are fed into the respective moulin (which is positioned at the lowest point of the elevation band), forming the input to the hydrological model. Model results are insensitive to the number and spacing of the moulins.

Results and Discussion

MASS BALANCE, ICE THICKNESS, AND TERMINUS POSITION

To put the results of the annual velocity measurements into perspective, we first describe the changes in glacier geometry that occurred during the decade 2000–2012, and the model estimates of the mass balance that drove these changes. In agreement with Anderson and others (2006), who used a degree-day model, the modeled mean annual mass balance varies from a little more than 5 m a^{-1} w.e. at the head of the glacier to a maximum of 19 m a^{-1} w.e. at the terminus (Fig 3). Over these years, there have been large variations in mass balance and, consequently, ice thickness and terminus position. Modeled annual mass balance varied between –2.9 m w.e. in the 2001/2002 mass balance year, and +1.9 m w.e. in the year 2003/2004 (Fig. 4). The calculated mass balances are generally inversely correlated with observations of annual ELA made at nearby Salisbury Glacier by Chinn et al. (2012)—that is, years of higher ELA are years of less positive/more negative mass balance and vice versa—although the relative magnitude of variation is different.

The annual ELA record also shows that prior to 2000 there were three years with high or very high ELA at Salisbury Glacier, suggesting negative or highly negative mass balance at FJG. High ELAs in 1998 and 1999 were associated with the end of an almost continuous 1983–1999 advance at FJG. The change from advance to retreat was very rapid, with the lower glacier losing an average of 70 m thickness between its maximum in 1998 and 2001, followed by slower thinning to 2004 (Fig. 5, part a). However, positive mass balances from 2002/2003 to 2005/2006 (Fig. 4) were sufficient to drive another advance from 2004 to 2006 (Fig. 5, part b). Close to neutral balances from 2007/2008 to 2009/2010 brought the advance to a gradual halt, before the very negative mass balance in 2010/2011 caused an extremely rapid thinning (Fig. 4; Fig. 5, part c).

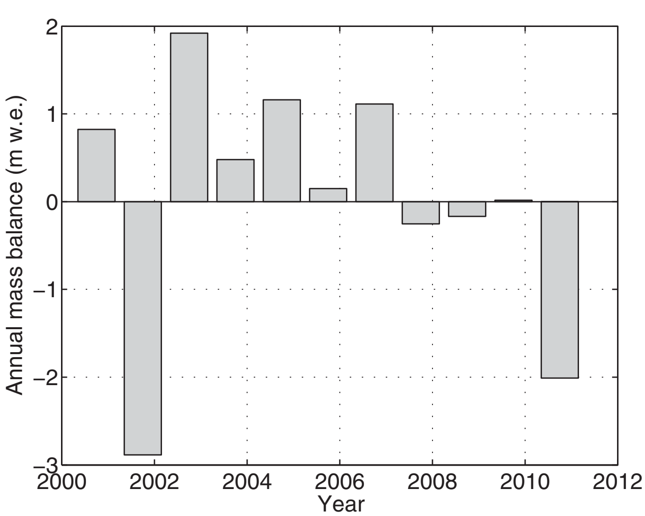

FIGURE 4. Annual mass balance, averaged over the glacier surface, for each year from 2000/2001 to 2010/2011.

VELOCITY VARIATION BETWEEN 2000 AND 2012

Velocity measurements between 2000 and 2012 (Fig. 6, part a) are collated from a variety of sources. Measurements between late 2000 and 2003 and those between late 2005 and 2012 were recorded as part of a long-term mass balance project. Additional velocity data have been drawn from the following sources: (*a*) GPS velocities collected between 3 August 2003 and 22 August 2003 (McClatchy, 2003); (*b*) average velocities measured close to stake 2 (stakes A, B, and C; see Fig. 1 for location) between 6 February 2004 and 18 February 2004; (*c*) velocities in January 2006 derived from feature tracking using repeat optical satellite imagery (Herman et al., 2011). Also shown in Fig. 6, part a, is glacier length, the derivative of which indicates whether the glacier is in a state of advance or retreat, and in Fig. 6, part b, we show ice thickness at stakes 2 and 3, a component of the local driving stress. The longitudinal cross-section geometry of the glacier terminus between 1998 and 2011 shown previously in Figure 5 can be used to help interpret Figure 6. Note from Figures 5 and 6 that ice at the lower stake 2 is thicker than that at the higher stake 3.

Velocities at stakes 2 and 3 show no clear pattern of increase or decrease between 2000 and 2003 (Fig. 6, part a). This is a period of glacier recession and general thinning (Figs. 5 and 6). A marked increase in velocity occurred at stake 2 between August 2003 and February 2004, just before the glacier started to advance (Fig. 6, part a). Another increase resulted in the highest velocity for the 2000–2012 period at stake 3 in January 2006, at the time of the maximum rate of advance (Fig. 5; Fig. 6, part a). The glacier thickened at stake 2 over these two time periods (Fig. 6, part b). Stake 2 velocity over this time interval was higher than that measured during 2000–2003, but similar to velocities measured in 2007–2008 (Fig. 6, part a). Between 2007 and 2012, the data show a general decrease in velocity, from >0.9 m d^{-1} in early 2007 to <0.5 m d^{-1} after June 2010 (Fig. 6, part a). This coincided with the glacier switching from an advancing state to a retreating phase (Fig. 5; Fig. 6, part a) and from a period of thickening to thinning (Fig. 5; Fig. 6, part b). By the latter part of 2011, stakes 2 and 3 were traveling at almost the same speed as one another. At the very end of the record, stake 2 sped up markedly and then became very slow. This was the result of the glacier dry calving into a large cavity near the terminus. Shortly after the last measurement, the ice at stake 2 calved into the cavity.

Thus, velocities on the tongue of FJG are typically higher when the glacier is advancing than when it is retreating. The simplest explanation for this is that the glacier tongue is both thicker and steeper when it is advancing, causing an increase in the driving stress. This requires an increase in basal shear stress to remain in force balance. This increase in basal shear stress is accommodated through an increase in basal motion, hence the observed increase in surface velocity (O'Neel et al., 2005). Conversely, the tongue is thinner and less steep as it retreats, driving stresses are lower, and velocities drop. This latter is what has been happening typically at glaciers in Europe and elsewhere, which have been thinning and slowing during the late 20th century (e.g., Hastenrath, 1987; Hambrey et al., 2005; Vincent et al., 2009).

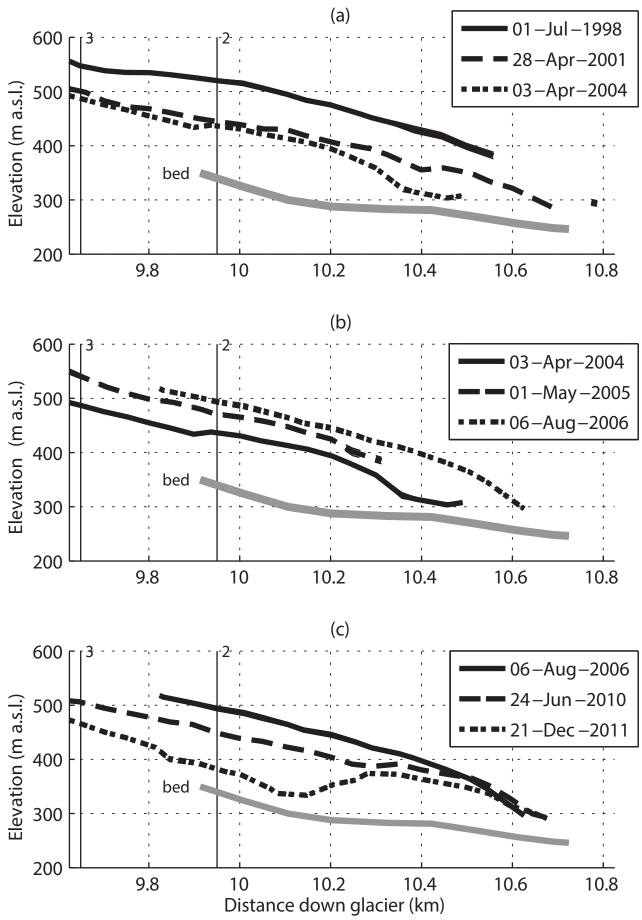

FIGURE 5. Geometry changes observed on the lower tongue of FJG, 1998 to 2011; (a) 1998 to 2004, (b) 2004 to 2006, and (c) 2006 to 2011. Thin lines above and below the surface elevation for each profile indicate the estimated errors in each profile, but are only visible when the errors are large. The positions of stakes 2 and 3 are shown with vertical lines.

However, the relationships between glacier velocity and advance/retreat at FJG are not so straightforward, and during the transitions from retreat to advance, and vice versa the timing of velocity, ice thickness, and terminus position changes can be counterintuitive. Nine months before the transition from retreat to advance, which occurred in November 2004 (Fig. 6, part a), ice velocity doubled at stake 2 (from 0.42 m d^{-1} in August 2003 to 0.96 m d^{-1} in February 2004). The terminus continued to retreat, and the first increase in ice thickness was not measured until April 2004–May 2005 (53 m over 13 months), although it may have started earlier. As the speed-up preceded advance, and possibly thickening as well, the forcing was not purely from local driving stress, but may have had a longitudinal component. Unfortunately, we do not have any velocity measurements at stake 3 over this period.

Between 2005 and 2008, the glacier continued to slowly thicken at stake 2 (10 m over three years), reaching a peak thickness in 2009. The glacier responded to the thickening by speeding up to the maximum velocities measured over the decade at stake 3 in January 2006, and the snout also advanced by 200 m from its 2004 position. Ice velocities were already decreasing in 2007, while the glacier was still thickening and advancing, and after 2008 the ice thinned at stakes 2 and 3. However, the snout continued to advance by >50 m between 2006 and 2008 before stablizing thereafter.

The behavior during these transitions between advance and retreat, and vice versa, is consistent with a kinematic wave of faster ice moving down the tongue through stakes 3 and 2 over the 2001 to 2004 period with compression ahead and extension behind the wave. The compression ahead of the faster ice meant that stake 2 sped up significantly before the glacier advanced, and perhaps before the ice thickened at that site. During 2005 to 2008, as in the 2001 to 2004 period, it appears as though there was a kinematic compression, then extension wave of faster velocity moving down glacier between 2004 and 2006.

To complete the story to 2012, although the terminus position is relatively stable up to early 2011, the glacier thinned very rapidly at stakes 2 (53 m in two years) and 3 (43 m in three years). Between January 2011 and February 2012, stake 2 thinned by a remarkable 54 m, and stake 3 by 39 m. The highest rate of thinning over this approximate one-year period was 70 m at 10.1 km from the head of the glacier (Fig. 5, part c). By 2012, the thin and uniform ice thickness and surface slope meant that stakes 2 and 3 moved at approximately the same velocity. The glacier thinned only slowly >10.3 km from the head of the glacier because it was protected by a thick layer of debris.

Thus, the data from FJG show that there is a fairly direct relationship between the local driving stress and ice velocity across the lower tongue, with increasing thickness correlated with increased speed. However, this is not always the case, and there are times (notably 2004 to 2005) when the glacier accelerates and longitudinal coupling is particularly noticeable. We have evidence for kinematic waves of faster moving ice moving down-glacier through the lower tongue, and the terminus advance (retreat) lags about a year behind the thickening/acceleration (thinning/deceleration) measured just 600 to 800 m up-glacier. The findings generally agree with those of previous studies (e.g., Span et al., 1997; Schlosser, 1997; Vincent et al., 2000; Span and Kuhn, 2003; Herman et al., 2011) showing that local ice thickness variations alone are not sufficient to explain annual variations in velocity.

HYDROLOGICAL MODEL OUTPUT

To help interpret the results of the seasonal, weekly, and daily glacier velocity measurements, we have calculated the subglacial water pressure variations along the length of the glacier using the methodology described earlier. Before we discuss the ice velocity and water pressure variations together and in detail, we first describe some of the general findings from our hydrological model in isolation.

Because of the idealized nature of the hydrological model, we are interested only in the spatial and temporal patterns of water pressure along the length of the glacier rather than its absolute magnitude. We have calculated daily patterns of conduit water discharge, cross-section area, water velocity, and water pressure along the length of the glacier between mass balance years 2000/2001 and 2010/2011, and we show typical results for one summer between 1 November 2003 and 28 March 2004 in Figure 7. Water discharge obviously increases from the headwall to the snout of the glacier but shows enormous temporal variability driven by patterns of melt and rainfall (Fig. 7, part a). Discharges range from <2 $m^3 s^{-1}$ to >14 $m^3 s^{-1}$ and can vary between these extremes within a few days. Water velocity varies along the length of the glacier with zones of relatively fast and slow flow and, like discharge, varies greatly through time

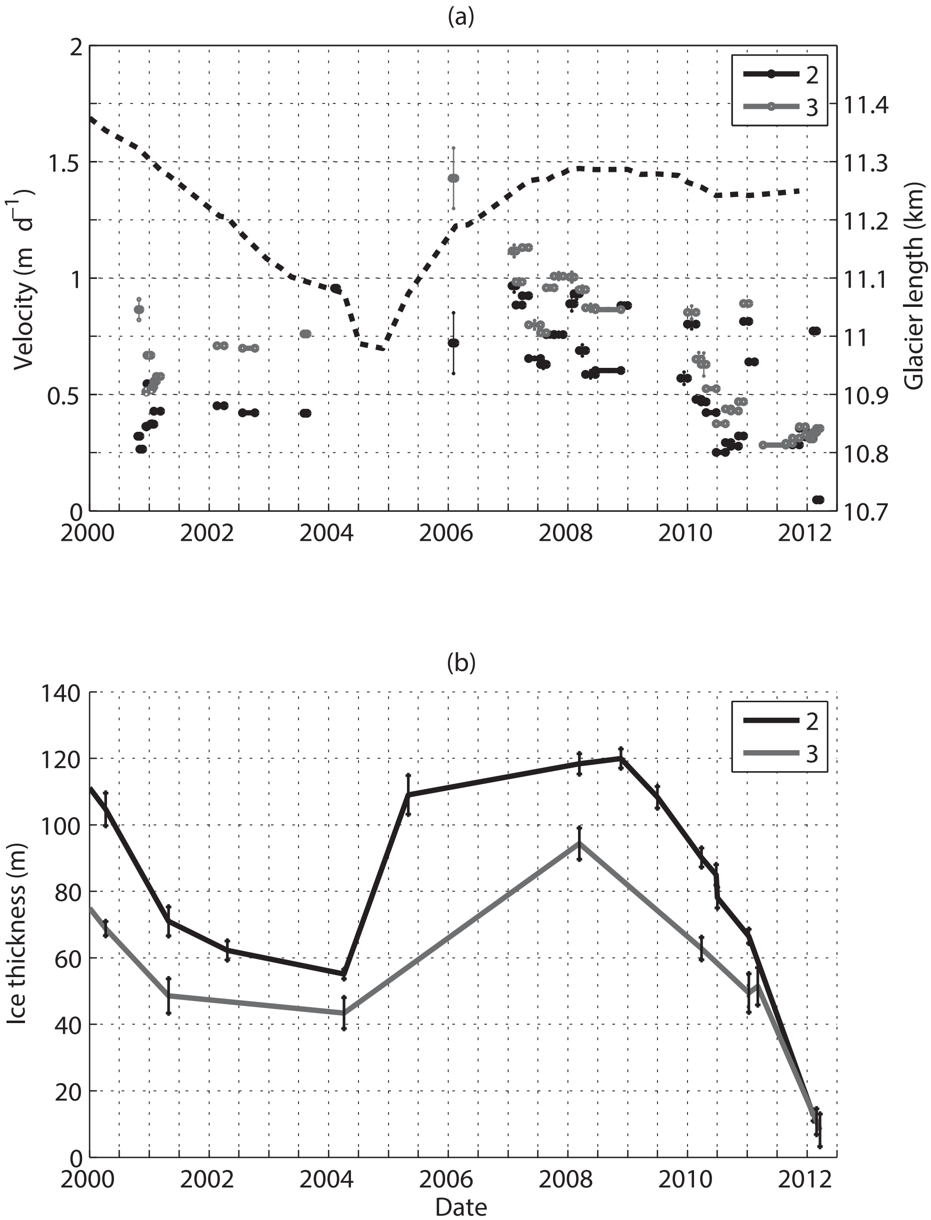

FIGURE 6. Twelve years of velocity and geometry change between 2000 and 2012. (a) Velocity variations at stakes 2 and 3. The thin vertical lines represent error estimates, but in many cases they are too small to see. The changing position of the glacier snout is shown as a dashed line. (b) Ice thickness variations at stakes 2 and 3, calculated from changes in their measured elevation and from the bed elevation determined by the mass flux method shown in Figure 2.

in response to water input variations (Fig. 7, part b). Water velocities reach maximum values of ~5 m s^{-1} in two zones at ~6 km and 7.5 km from the headwall during peaks in water input. Like velocity, conduit diameter also varies markedly down glacier (Fig. 7, part c); in some zones conduits remain relatively small (<3 m diameter) throughout the summer, whereas in other places, notably ~5 km, ~7.5 km, ~9.5 km, and ~10 km from the headwall, diameters exceed 8 m during late summer. Unlike water velocity and discharge, which respond rapidly to input variations, conduit diameters vary much more slowly in response to gradual adjustments associated with melt enlargement and creep closure. Water pressure also varies dramatically in space and time (Fig. 7, part d). Although pressures are at or close to atmospheric beneath much of the glacier for most of the time, there are short-lived pulses of rapidly varying pressure, from atmospheric to over ice overburden and back again in a few days, associated with variations in meltwater input. Pressurized zones are confined to just three places, centered on ~2 km, 6.5 km, and, for a short period in early summer, ~10.5 km from the headwall when meltwater inputs are high but conduit diameters are small (Fig. 7, part c). The average and maximum water pressures over the 2003/2004 summer are plotted in Figure 2, confirming that the zones susceptible to pressure fluctuations are the overdeepenings (as well as the entire glacier tongue, although here it is just for a few days in early summer). Hooke (1984) also found from theoretical considerations that steady-state water pressures in conduits may be at or close to atmospheric where discharges are large, gradients are high, and ice is thin. In the overdeepenings on FJG, where gradients are shallower and ice is thicker than elsewhere, rates of conduit enlargement are relatively low and rates of closure are relatively high, giving smaller conduit diameters and higher long-term average water pressures throughout the summer (Fig. 7, parts c and d). These findings are similar to observations made on other thin, steep alpine glaciers in the summer, where borehole water-level readings indicate that close to channels, water pressures regu-

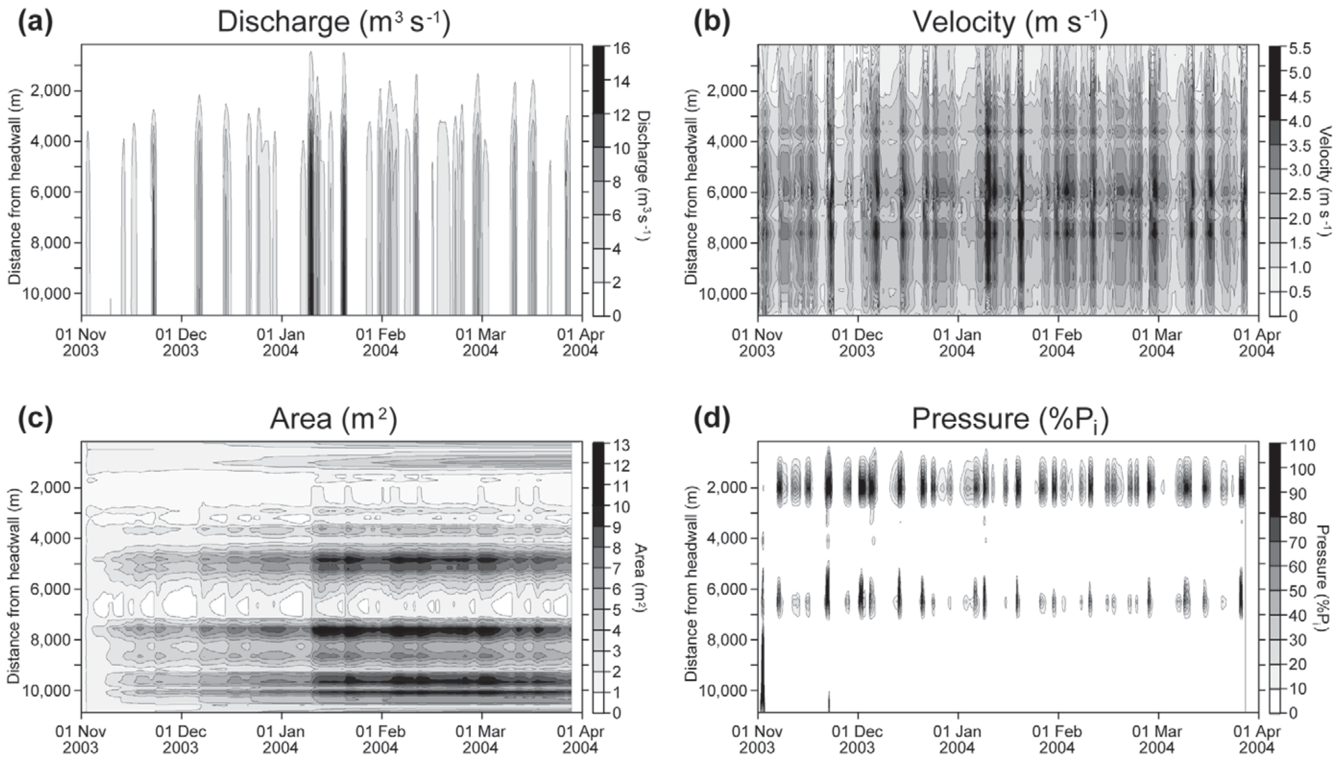

FIGURE 7. Plots showing subglacial hydrological model output along the glacier centerline between 01 November 2003 and 01 April 2004: (a) water discharge; (b) water velocity; (c) conduit cross-section area; and (d) water pressure. The unit '$\%P_i$' represents water pressure as a percentage of ice overburden at each site.

larly drop to atmospheric or near atmospheric but rise during times of rapid water inputs (Engelhardt et al., 1978; Fountain, 1994; Hubbard et al., 1995).

SEASONAL VARIATIONS

Figure 8 shows the velocities measured at stakes 2 and 3 (location in Fig. 1), together with glacier surface water inputs from melt and rain over a two-year period from January 2007 to December 2008. For both stakes in both years, high velocities are measured from January to April, and lowest speeds occur between May and August. Thus, the glacier flows faster in the summer months than during the winter. In spring 2007 (September to November), the higher elevation stake 3 appears to be in the "summer regime" with velocities comparable to those measured from January to April, whereas the lower stake 2 seems to be part way between its "winter" and "summer" regimes, with velocities intermediate between those measured in the seasons on either side. We have no data for December. The summer and winter velocities for these two stakes are presented in Table 2. Average summer velocities are 39% greater than winter velocities at stake 2. At stake 3, the corresponding figure is 23%.

The seasonal velocity pattern generally mimics the seasonal pattern of water inputs with maximum (minimum) velocities coinciding with maximum (minimum) water inputs (Fig. 8). The spring 2007 data show that the "summer regime" (at stake 3) and the "intermediate regime" (at stake 2) occur as water inputs are rising from <10 m^3 s^{-1}. While there is no clear seasonality to rainfall events, there is a clear seasonality in water inputs, which includes melt. The clear relationships between water inputs and velocity are reflected in the strength of the correlations between these variables (Table 3), where both stake 2 and 3 show a statistically significant relationship. Additionally, stake 2 shows a significant relationship with temperature, and stake 3 with rainfall.

At this temporal scale, there is an inverse relationship between subglacial water flux and water pressure along the length of the glacier, with the higher melt rates associated with the higher air temperatures in the summer, corresponding with water pressures that are generally a lower fraction of ice overburden than in the winter, when air temperatures and melt rates are lower. This is particularly obvious in the overdeepening between 5.3 km and 6.9 km from the head of the glacier (Fig. 8, part b). Average water pressures drop in the summer as the conduits enlarge by wall melting to accommodate the extra water flux (cf. Fig. 7, parts a and d). However, short-term variability in water pressure is high in the summer, with water pressures rising from <40% ice overburden to >80% ice overburden over a day or a few days on several occasions associated with rapid increases in water inputs (Fig. 8). This is particularly obvious during the rapid rise in water inputs associated with the rainstorm in mid-December 2007 causing a water pressure pulse from 50% overburden to >100% overburden in a day. In winter, average water pressures go up as the conduits shrink by ice deformation in response to the reduced water flux (cf. Fig. 7, parts a and d). In winter, pressures tend to be sustained at high values for long periods of time and there is relatively little short-term variability in water pressure (Fig. 8).

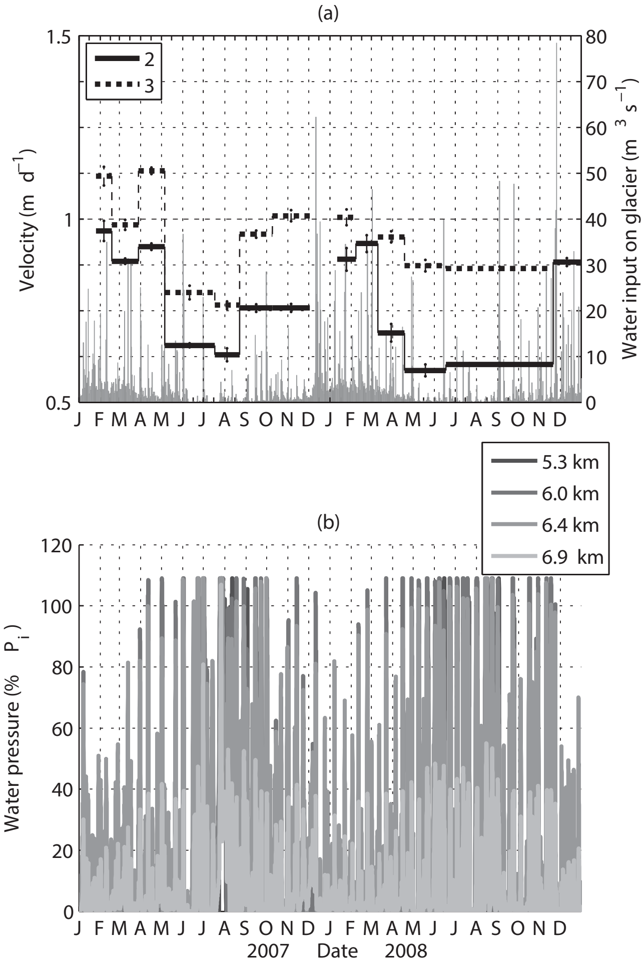

FIGURE 8. (a) Seasonal velocity variations of stakes 2 and 3 together with surface water inputs calculated from the mass balance model, January 2007 to December 2008. The dates on the x-axis are positioned at the start of each year. (b) Water pressure variations determined from the hydrological model in moulins located different distances from the headwall shown in Figure 2. Water pressure variations occurred in all 23 moulins although was atmospheric for most of the time in only five of them. Pressures in only four moulins are shown for clarity.

TABLE 2

Summer and winter velocities measured at stakes 2 and 3 over a period of two years.

	Velocity (m d^{-1})			
Stake	Summer 2006/2007	Winter 2007	Summer 2007/2008	Winter 2008
2	0.92	0.68	0.85	0.60
3	1.09	0.78	0.95	0.88

An increase in summer over winter velocities of 36% was measured on the tongue of nearby Fox Glacier in 2005 (Purdie et al., 2008) and is in this respect similar to the 20% to 40% summer increase measured at FJG. Seasonal variations in velocity, with spring/summer velocities greater than those in autumn/winter, have been measured on many glaciers (see Willis, 1995, for a review) and most are comparable in magnitude to those observed on FJG. We interpret the relationship between warmer summer temperatures and higher velocities at FJG in the same way as others have done on other glaciers, notably that higher temperatures are associated with higher ablation, creating higher inputs of water to the glacier bed, resulting in reduced basal friction, and thus seasonally enhanced basal motion (e.g., Bindschadler et al., 1977; Iken and Bindschadler, 1986; Clarke, 1991; Jansson, 1995; Willis, 1995; Rippin et al., 2005).

TABLE 3

Pearson's linear correlation coefficient and significance of measured ice velocity against rainfall, temperature, and total water inputs to Franz Josef Glacier. The numbers in the table are correlation coefficients, and the numbers in bold are also significant at the 5% level in a single-tailed Pearson test.

Period	Stake	Rainfall	Temperature	Total water inputs
5–19 Feb 2004	A	–0.02	0.29	0.33
	B	–0.05	**0.60**	–0.43
	C	–0.04	0.25	**0.55**
1 Oct 2000–28 Feb 2001	2	**0.96**	0.46	**0.91**
	3	–0.55	0.20	–0.33
	5	0.47	0.44	0.48
	6	**0.92**	–0.04	0.51
	7	**0.85**	–0.06	0.48
1 Jan 2007–31 Dec 2008	2	0.12	**0.83**	**0.77**
	3	**0.75**	–0.25	**0.67**

The relationship between measured ice velocities and calculated water pressures at this seasonal time scale confirms the results of observations and modeling made elsewhere, that it is the variability in water pressure more than its absolute magnitude that is important in reducing basal friction and driving basal movement (Iken, 1981; Schoof, 2010; Colgan et al., 2011; Bartholomew et al., 2012).

The general decrease in velocities over 2007 and 2008 is interpreted in terms of the overall thinning and retreat of the glacier; this concept was investigated in the previous section.

WEEKLY VARIATIONS

Weekly variations in spring and summer velocities were measured at five locations—stakes 2, 3, 5, 6, and 7 (location in Fig. 1)—between October 2000 and February 2001 and are shown alongside glacier surface water inputs from melt and rain in Figure 9, part a. Velocities increase with distance up glacier, although all five stakes generally show the same temporal variations in velocity. There are significant velocity variations over the five months, with four periods of high velocity (late October, late November, late December–early January, and early February) interspersed with periods of low velocity. The biggest jump in velocity occurs in November when stakes 6 and 7 increase by over 100% from just over 0.6 m d^{-1} during early November to >1.2 m d^{-1} during late November (Fig. 9, part a).

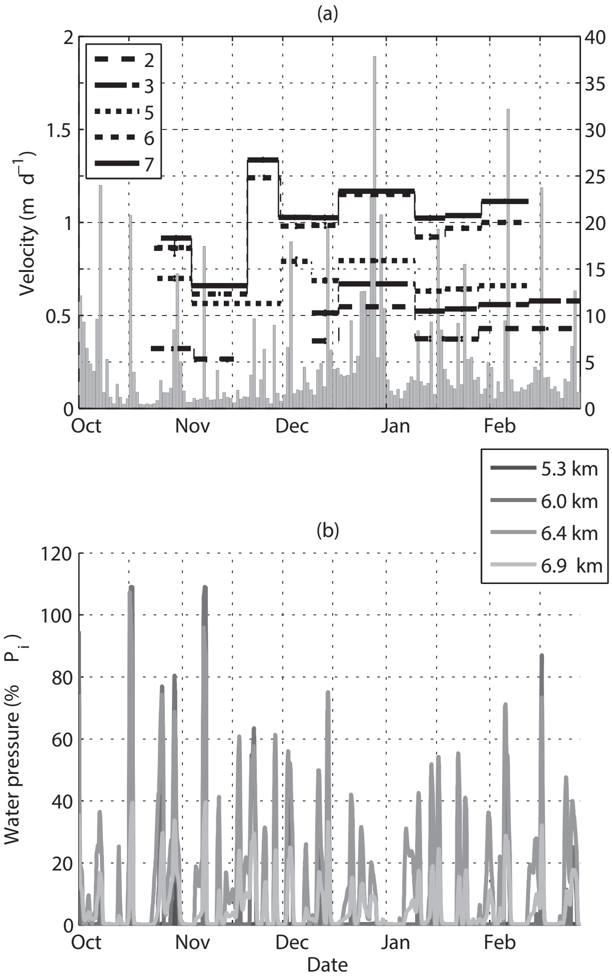

FIGURE 9. (a) Subseasonal velocity variations measured at stakes 2, 3, 5, 6, and 7 together with surface water inputs calculated from the mass balance model, from October 2000 to February 2001. (b) Water pressure variations determined from the hydrological model in moulins located different distances from the headwall shown in Figure 2. Water pressure variations occurred in 15 of the 23 moulins and remained at atmospheric in the remaining 8 moulins. Pressures in only 4 moulins are shown for clarity.

This late November period of fast motion occurs at a time of frequent pulses in surface water inputs to the glacier surface associated with the first significant air temperature rise of the spring and a number of rainstorms following a period of about three weeks with very little rain. There are four pulses of high subglacial water pressure associated with these water inputs that are particularly marked in the overdeepening between 5.3 km and 6.9 km from the head of the glacier (Fig. 9, part b). Two of the pulses have water pressures of >60% ice overburden. The late December–early January period of fast motion affects all five stakes; velocities are higher by ~0.2 m d^{-1} compared with the time periods before and after. This period is associated with a progressive rise in water inputs linked with rising air temperatures and increases in melt rates, together with marked pulses of water inputs linked to large rainstorms. There are four pulses of high subglacial water pressure over this late December–early January period in the overdeepening 5.3 km to 6.9 km from the headwall (Fig. 9, part b). Despite the higher volumes of water inputs during this period compared to the late November period, the pressure pulses are less marked, reaching only 20%–40% of ice overburden. This is because the subglacial conduits have adjusted to the higher water fluxes flowing through them; they have enlarged and water is flowing at lower pressures.

The two stakes with the best-resolved velocity measurements for the period (stakes 6 and 7) show a significant relationship with rainfall (Table 3). Stake 2 shows a significant relationship with both rainfall and total water inputs.

The particularly high velocities in late November 2000 at stakes 6 and 7, coinciding with the first significant temperature rise of the summer, together with several days of moderate rainfall following a few weeks of negligible rainfall are, in this respect, similar to the first "spring event" of 1998 measured on Haut Glacier d'Arolla, which was also driven by an increase in meltwater and rainwater inputs to the subglacial drainage system at the start of the summer (Mair et al., 2003). Like observations on Haut Glacier d'Arolla, the FJG November 2000 speed-up appears to mark the switch from a "winter" to a "summer" velocity regime, with velocities at all stakes after the event consistently higher than those before. "Spring events" marking the onset of faster summer sliding have been reported from many glaciers and are interpreted as representing the first significant increases in surface water inputs to a subglacial drainage system that is hydraulically inefficient as a result of shrinkage due to low discharges and creep closure during the winter. They mark the first significant pulses of high subglacial water pressure over the glacier bed, hydraulic jacking, reduced bed friction, and increased basal motion (Iken et al., 1983; Röthlisberger and Lang 1987; Mair et al. 2001, 2003). Comparable events have recently been observed on Russell/Leveret Glacier, an outlet glacier complex on the west side of the Greenland Ice Sheet (Bartholomew et al., 2010). A key difference between FJG and the other glaciers mentioned above is that the FJG tongue generally remains snow-free throughout the winter, and air temperatures over the tongue remain mostly above freezing. As far as we know, this is the first time a spring event has been reported for a New Zealand glacier, and for a glacier for which surface water inputs are fed to the subglacial drainage system throughout the winter. There is a possibility that a second "event," comparable in duration and magnitude to the first, occurred during the period of rainfall lasting several days in late December 2000, although the resolution of our measurements at this time do not allow us to conclude this with certainty. The lower water pressures during this time period suggest this may not, however, be the case (Fig. 9, part b).

DAILY VARIATIONS

Surveys to stakes A, B, and C close to stake 2 (location in Fig. 1) were made almost every day from 6 to 18 February 2004 and are presented alongside surface water inputs from melt and rain in Figure 10, part a. There is a decreasing trend in velocity at all three stakes during the 12-day period, interrupted by short-term velocity increases/decreases. The average velocities for stakes A, B, and C were 1.06, 1.0, and 0.99 m d^{-1}, respectively; for each stake, velocity variations over the 12-day period were within 0.4 m d^{-1} of the stake's average velocity, except for the biggest short-term increase of the period on 10 February during which stake C increased by 0.6 m d^{-1}, or 65% above the mean.

Water inputs to the glacier are fairly low and constant over the period. Notable exceptions are the large volumes of water inputs on 10 February driven by an intense rainstorm, and moderate

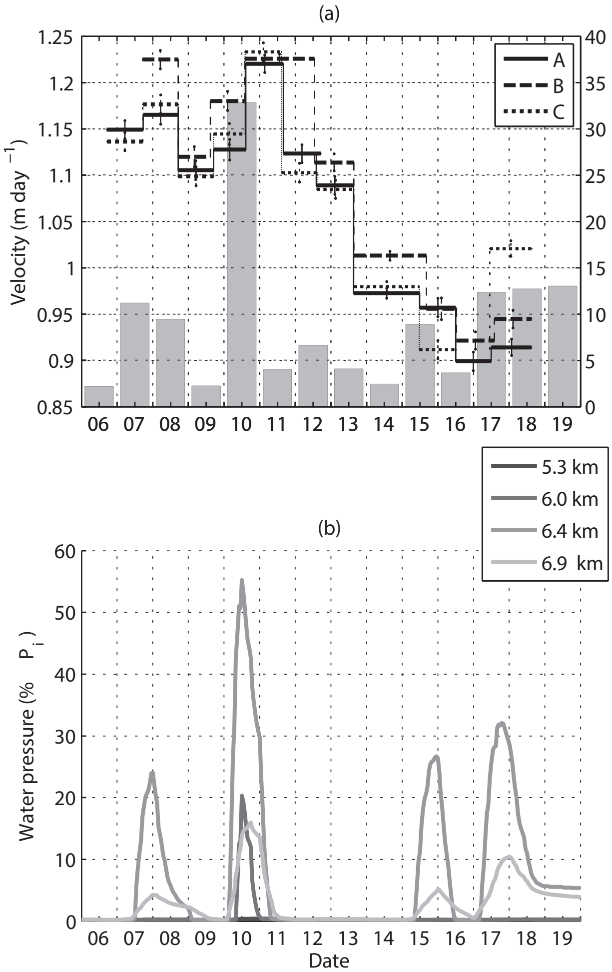

FIGURE 10. (a) Daily velocity variations for stakes A, B, and C together with surface water inputs calculated from the mass balance model, February 2004. (b) Water pressure variations determined from the hydrological model in moulins located different distances from the headwall shown in Fig. 2. Water pressure variations occurred in 5 of the 23 moulins and remained at atmospheric in the remaining 18 moulins. Pressures in only 4 moulins are shown for clarity.

volumes on 7 and 8 February driven by less intense rainstorms, and on 15, 17, 18, and 19 February driven by large diurnal melt cycles. Thus, velocities appear to be linked with surface water inputs, especially toward the beginning of the time period. We find generally weak correlations, although temperature and stake B velocity, and water inputs and stake C velocity, are significantly correlated (Table 3).

The hydrological model results show that water pressures are largely atmospheric beneath most of the glacier for most of the time during this period of late summer (Fig. 10, part b). However, the rainstorms on 7 and 10 February and the diurnal melt cycles on 15 and 17 February produce water pressure fluctuations that are particularly marked in the overdeepening between 5.3 km and 6.9 km from the head of the glacier where pressures reach up to 55% of ice overburden (Fig. 10, part b). The diurnal melt cycles on 18 and 19 February do not produce marked water pressure fluctuations since the conduits have enlarged as a result of the inputs on 17 February and are able to accommodate the water that flows at lower pressures (Fig. 10, part b).

Thus, at least during February 2004, the glacier is particularly sensitive to high magnitude rainfall events, with velocities responding quickly (<1 day) to the rain inputs. McSaveney and Gage (1968) also identified daily variations in velocity across the FJG tongue from their measurements in May and August 1966 with some of the largest increases in velocity associated with rainstorms. Similarly, Purdie et al. (2008) observed daily velocity variations at nearby Fox Glacier during both January/February 2005 and June/July 2005. As at FJG, the greatest velocity variations at this time scale were in response to rainfall events, and responses were also rapid (<1 day).

Outside New Zealand, other workers have reported short-term increases in velocity in response to rainstorms. On Hansbreen, Svalbard, a short-term speed-up in June occurred in response to a small (10 mm in 18 hours) rainfall event (Vieli et al., 2004). Similarly, Mair et al. (2003) reported a June speed-up event following rainfall (>25 mm in 24 hours) at Haut Glacier d'Arolla, Switzerland. From measurements on several glaciers, it appears that speed-up events are less common later in the summer unless rainstorms are particularly large, and/or follow several days to weeks of declining water inputs giving the subglacial drainage system time to shrink in response to ice creep. Such phenomena have been reported from Unteraargletscher, Switzerland (Flotron, unpublished data, cited in Iken and Bindschadler, 1986); Storglaciaren, Sweden (Hooke et al., 1989); Midtdalsbreen, Norway (Willis, 1995); and Bench Glacier, USA (Fudge et al., 2009). Similarly, although not measured at such a high temporal resolution, Sund et al. (2011) found the average September velocity of Kronebreen, Svalbard, in 2008 was higher than the average June–August velocity. This contrasted with the typical situation in other years where September velocities are lower than average, but was attributed to unusually large rainstorms in September 2008.

Conclusions

Observations over a decade of ice velocity, surface elevation, and terminus position, combined with modeled surface mass balance and subglacial water pressure at FJG show a remarkably rapid and significant reaction to climatic and hydrological drivers. Ice on the lower glacier can thin or thicken at rates of up to 50 m a^{-1}. Over a decade, this results in velocities that vary between 0.25 and 1.5 m d^{-1} at our measurement sites, while the temporal pattern of change is consistent with the effects of kinematic waves moving down-glacier. Seasonal velocity variations measured over two years are similar at FJG to those measured at other glaciers, with ~20% and ~40% summer increases at our measurement sites. Weekly velocity variations measured over five months are particularly marked, with up to 100% increases associated with rises in air temperature and large rainfall events.

Addressing the four hypotheses that we set out at the beginning of our study:

1. The distinctive pattern of recent climate change over the Southern Alps, resulting in glacier advance as well as retreat, has caused greater annual variability in velocity at FJG compared to many glaciers elsewhere which have simply undergone terminus retreat and slowdown. The changes in ice thickness and terminus position are large and rapid, a result of the relatively high mass turnover of this glacier (Anderson and Mackintosh, 2012) and the narrow tongue.

2. Despite the glacier tongue remaining snow-free in the winter and the year-round abundance of meltwater and rainwater, seasonal variations in subglacial water pressure do occur at FJG and seasonal glacier velocity variations are not necessarily more limited on FJG than elsewhere. The seasonal variations in surface melt are sufficient to drive seasonal changes in the hydraulic efficiency of the subglacial drainage system. Average water pressures in a conduit system drop during the summer, but summer velocities are higher than in the winter due to greater variability of water inputs.
3. Despite the year-round abundance of meltwater and rainwater, there does appear to be evidence of a period of fast movement on FJG similar in timing to the "spring event" observed on other glaciers, with high velocities in late November (equivalent to late May in the North Hemisphere) coinciding with the first significant temperature rise of the summer and a period of moderate rainfall. The "spring event" at FJG also appears to mark a switch from a "winter" to a "summer" velocity regime, as recorded elsewhere. The reduced water inputs to the glacier in winter are sufficient to allow the subglacial drainage system to reduce its capacity so fluctuations in subglacial water pressure sufficient to trigger a "spring event" do occur beneath FJG.
4. The limited daily radiation and temperature range and variability over glaciers in the Southern Alps do appear to result in little daily velocity variation on FJG, although rainstorms are particularly significant in producing short-term increases in speed.

A decade of observations on FJG show that its speed fluctuates at a variety of time scales. Daily increases in speed in response to rainfall events, "spring events," and faster flow in the summer than in the winter all show that hydrological drivers are important on this glacier. Despite the simplicity of our one-dimensional channelized hydrological model, it is capable of reproducing spatial and temporal patterns of subglacial water pressures that seem sensible in the context of the observed velocity variations, with high pressures concentrated in the overdeepening ~5–7 km from the snout and at times of rapid water inputs. However, due to the lack of a distributed component, our model likely underestimates the places and times experiencing high pressures, and likely predicts atmospheric pressures beneath too much of the glacier for too much of the year.

Acknowledgments

We thank the many former students (too numerous to mention individually) from the Universities of Canterbury and Victoria who have helped with fieldwork at FJG over the years. We also thank David Chandler for help collecting the summer 2004 data. Some of the work for this paper was undertaken while Ian Willis was a visiting scholar at the University of Canterbury, and he thanks all the staff there for their hospitality. We thank Phil Stickler at the Department of Geography, University of Cambridge, for help drafting the figures.

References Cited

Anderson, B., and Mackintosh, A., 2012: Controls on mass balance sensitivity of maritime glaciers in the Southern Alps, New Zealand: the role of debris cover. *Journal of Geophysical Research: Earth Surface,* 117 (F1), doi: http://dx.doi.org/10.1029/2011JF002064.

Anderson, B., Lawson, W., Owens, I., and Goodsell, B., 2006: Past and future mass balance of Ka Roimata o Hine Hukatere (Franz Josef Glacier). *Journal of Glaciology*, 52(179): 597–607.

Anderson, B. M., Lawson, W. J., and Owens, I. F., 2008: Response of Franz Josef Glacier Ka Roimata o Hine Hukatere to climate change. *Global and Planetary Change,* 63: 23–30.

Anderson, B., Mackintosh, A., Stumm, D., George, L., Kerr, T., Winter-Billington, A., and Fitzsimons, S., 2010: Climate sensitivity of a high-precipitation glacier in New Zealand. *Journal of Glaciology*, 56(195): 114–128.

Arnold, N., Richards, K., Willis, I., and Sharp, M., 1998: Initial results from a distributed, physically based model of glacier hydrology. *Hydrological Processes*, 12: 191–219.

Banwell, A. F., Arnold, N., Willis, I., Tedesco, M., and Ahlstrom, A., 2012: Modeling supraglacial water routing and lake filling on the Greenland Ice Sheet. *Journal of Geophysical Research—Earth Surface,* 117, F0401, doi: http://dx.doi.org/10.1029/2012JF002393.

Banwell, A. F., Willis, I., and Arnold, N., 2013: Modeling subglacial water routing at Paakitsoq, W Greenland. *Journal of Geophysical Research—Earth Surface,* 118*,* doi: http://dx.doi.org/10.1002/jgrf.20093.

Bartholomew, I., Nienow, P., Mair, D., Hubbard, A., King, M., and Sole, A., 2010: Seasonal evolution of subglacial drainage and acceleration in a Greenland outlet glacier. *Nature Geoscience*, 3: 408–411.

Bartholomew, I., Nienow, P., Sole, A., Mair, D., Cowton, T., and King, M. A., 2012: Short-term variability in Greenland Ice Sheet motion forced by time-varying meltwater drainage: implications for the relationship between subglacial drainage system behavior and ice velocity. *Journal of Geophysical Research,* 117, F03002, doi: http://dx.doi.org/10.1029/2011JF002220.

Bindschadler, R., Harrison, W. D., Raymond, C. F., and Crosson, R., 1977: Geometry and dynamics of a surge-type glacier. *Journal of Glaciology*, 18(79): 181–194.

Chinn, T., Fitzharris, B. B., Willsman, A., and Salinger, M. J., 2012: Annual ice volume changes 1976–2008 for the New Zealand Southern Alps." *Global and Planetary Change* 92-93(July): 105–118, http://dx.doi.org/10.1016/j.gloplacha.2012.04.002.

Clarke, T. S., 1991: Glacier dynamics in the Susitna River basin, Alaska, USA. *Journal of Glaciology*, 37(125): 97–106.

Colgan, W., Rajaram, H., Anderson, R., Steffen, K., Phillips, T., Joughin, I., Zwally, J. H., and Abdalati, W., 2011: The annual glaciohydrology cycle in the ablation zone of the Greenland Ice Sheet: Part 1. Hydrology model. *Journal of Glaciology,* 57(204): 697–709, doi: http://dx.doi.org/10.3189/002214311797409668.

Engelhardt, H. F., Harrison, W. D., and Kamb, B., 1978: Basal sliding and conditions at the glacier bed as revealed by bore-hole photography. *Journal of Glaciology*, 20: 469–508.

Farinotti, D., Huss, M., Bauder, A., Funk, M., and Truffer, M., 2009: A method to estimate the ice volume and ice thickness distribution of alpine glaciers. *Journal of Glaciology*, 55(191): 422–430.

Fountain, A. G., 1994: Borehole water-level variations and implications for the subglacial hydraulics of South Cascade Glacier, Washington State, U.S.A. *Journal of Glaciology,* 40: 293–304.

Fudge, T. J., Harper, J. T., Humphrey, N. F., and Pfeffer, W. T., 2009: Rapid glacier sliding, reverse ice motion and subglacial water pressure during an autumn rainstorm. *Annals of Glaciology,* 50(52): 101–108, doi: http://dx.doi.org/10.3189/172756409789624247.

GLIMS and NSIDC, 2005: GLIMS Glacier Database, New Zealand Subset. Boulder, Colorado: National Snow and Ice Data Center, updated 2012. http://dx.doi.org/10.7265/N5V98602.

Griffiths, G. A., and McSaveney, M. J., 1983: Distribution of mean annual precipitation across some steepland regions of New Zealand. *New Zealand Journal of Science*, 26: 197–209.

Grove, J. M., 2004: *Little Ice Ages, Ancient and Modern*. Second edition. London and New York: Routledge.

Gunn, B. M., 1964: Flow rates and secondary structures of Fox and Franz Josef Glaciers, New Zealand. *Journal of Glaciology*, 5(38): 173–190.

Hambrey, M. J., Murray, T., Glasser, N.F., Hubbard, A., Hubbard, B., Stuart, G., Hansen, S., and Kohler J., 2005: Structure and changing dynamics of a polythermal valley glacier on a centennial timescale: Midre Lovenbreen, Svalbard. *Journal of Geophysical Research*, 110: F01006.

Hastenrath, S., 1987: On the relation of net balance, ice flow, and surface lowering of Lewis Glacier, Mount Kenya, 1982–86. *Journal of Glaciology*, 33(115): 315–318.

Herman, F., Anderson, B., and Leprince, S., 2011: Mountain glacier velocity variation during a retreat/advance cycle quantified using sub-pixel analysis of ASTER images. *Journal of Glaciology*, 57(202): 197–207.

Hooke, R. Le B., 1984: On the role of mechanical energy in maintaining subglacial conduits at atmospheric pressure. J. Glaciology, 30 (105): 180-87.

Hooke, R. Le B., Calla, P., Holmlund, P., Nilsson,M., and Stroeven, A., 1989: A three year record of seasonal variations in surface velocity, Storglaciären, Sweden. *Journal of Glaciology*, 35(120): 235–247.

Hubbard, B., Sharp, M., Willis, I. C., Nielsen, M. K., and Smart, C. C., 1995: Borehole water-level variations and the structure of the subglacial hydrological system of Haut Glacier d'Arolla, Valais, Switzerland. *Journal of Glaciology*, 41(139): 572–583.

Iken, A., 1981: The effect of the subglacial water pressure on the sliding velocity of a glacier in an idealized numerical model. *Journal of Glaciology,* 27(97), 407–421.

Iken, A., and Bindschadler, R. A., 1986: Combined measurements of subglacial water pressures and surface velocity of the Findelengletscher, Switzerland. Conclusions about drainage systems and sliding mechanism. *Journal of Glaciology*, 32(110): 101–119.

Iken, A., Röthlisberger, H., Flotron, A., and Haeberli, W., 1983: The uplift of Unteraargletscher at the beginning of the melt season—a consequence of water storage at the bed? *Journal of Glaciology,* 29(101): 28–47.

Ishikawa, N., Owens, I. F., and Sturman, A. P., 1992: Heat balance characteristics during fine periods on the lower parts of the Franz Josef Glacier, South Westland, New Zealand. *International Journal of Climatology,* 12(4): 397–410, doi: http://dx.doi.org/10.1002/joc.3370120407.

Jansson, P., 1995: Water pressure and basal sliding on Storglaciären, northern Sweden. *Journal of Glaciology*, 41(138): 232–240.

Leclercq, P., and Oerlemans, J., 2011: Global and hemispheric temperature reconstruction from glacier length fluctuations. *Climate Dynamics,* 38(5-6): 1065–1079.

Mair, D., Nienow, P., Willis, I., and Sharp, M., 2001: Spatial patterns of glacier motion during a high-velocity event: Haut Glacier d'Arolla, Switzerland. *Journal of Glaciology*, 47(156): 9–20.

Mair, D., Willis, I., Fischer, U., Hubbard, B., Nienow, P., and Hubbard, A., 2003: Hydrological controls on patterns of surface, internal and basal motion during three "spring events": Haut Glacier d'Arolla, Switzerland. *Journal of Glaciology*, 49(167): 555–567.

McClatchy, H., 2003: *Velocities, Strain Fields and Structure: Spatial Flow Characteristics of the Franz Josef Glacier, Southern Alps, New Zealand.* Undergraduate dissertation, Department of Geography, University of Canterbury, Christchurch, New Zealand.

McSaveney, M. J., and Gage, M., 1968: Ice flow measurements on Franz Josef Glacier, New Zealand, in 1966. *New Zealand Journal of Geology and Geophysics,* 11(3): 564–592.

O'Neel, S., Pfeffer, W. T., Krimmel, R., and Meier, M., 2005: Evolving force balance at Columbia Glacier, Alaska, during its rapid retreat. *Journal of Geophysical Research,* 110, F03012, doi: http://dx.doi.org/10.1029/2005JF000292.

Owens, I. F., Marcus, M. G., and Moore, R. D., 1984: Temporal variations of the energy transfers over the lower part of the Franz Josef Glacier. *In* Proceedings of the 12th Conference of the New Zealand Geographical Society, 83–87.

Purdie, H. L., Brook, M. S., and Fuller, I. C., 2008: Seasonal variation in ablation and surface velocity on a temperate maritime glacier: Fox Glacier, New Zealand. *Arctic, Antarctic, and Alpine Research*, 40(1): 140–147.

Rippin, D. M., Willis, I. C., Arnold, N. S., Hodson, A. J., and Brinkhaus, M., 2005: Spatial and temporal variations in surface velocity and basal drag across the tongue of the polythermal Midre Lovénbreen, Svalbard. *Journal of Glaciology*, 51(175): 588–600.

Roesner, L. A., Aldrich, J. A., and Dickinson, R. E., 1988: *Storm Water Management Model User's Manual, Version 4; EXTRAN addendum.* Athens, Georgia: U.S. Environmental Protection Agency, 188 pp.

Röthlisberger, H., and Lang, H., 1987: Glacial hydrology. *In* Gurnell, A. M., and Clarke, M. J. (eds.), *Glacio-fluvial Sediment Transfer: An Alpine Perspective*. London: Wiley, 207–284.

Schlosser, E., 1997: Numerical simulation of fluctuations of Hintereisferner, Ötztal Alps, since AD 1850. *Annals of Glaciology*, 24: 199–202.

Schoof, C., 2010: Ice-sheet acceleration driven by melt supply variability. *Nature,* 468: 803–806.

Span, N., and Kuhn, M., 2003: Simulating annual glacier flow with a linear reservoir model. *Journal of Geophysical Research*, 108(D10): 4313, doi: http://dx.doi.org/10.1029/2002JD002828.

Span, N., Kuhn, M., and Schneider, H., 1997: 100 years of ice dynamics of Hintereisferner, Central Alps, Austria, 1894–1994. *Annals of Glaciology*, 24: 297–302.

Spring, U., and Hutter, K., 1981: Numerical studies of jökulhlaups. *Cold Regions Science and Technology*, 4: 227–244.

Sund, M., Eiken, T., and Denby, R., 2011: Velocity structure, front position changes and calving of the tidewater glacier Kronebreen, Svalbard. *The Cryosphere Discussions*, 5: 41–73.

Tait, A. B., and Turner, R. W., 2005: Generating multi-year gridded daily rainfall over New Zealand. *Journal of Applied Meteorology*, 44: 1315–1323.

Vieli, A., Jania, J., Blatter, H., and Funk, M., 2004: Short-term velocity variations on Hansbreen, a tidewater glacier in Spitsbergen. *Journal of Glaciology*, 50(170): 389–398.

Vincent, C., Vallon, M., Reynaud, L., and Le Meur, E., 2000: Dynamic behaviour analysis of glacier de Saint Sorlin, France, from 40 years of observations, 1957–1997. *Journal of Glaciology*, 46(154): 499–506.

Vincent, C., Soruco, A., Six, D., and Le Meur, E., 2009: Glacier thickening and decay analysis from 50 years of glaciological observations performed on Glacier d'Argentiere, Mont Blanc area, France. *Annals of Glaciology*, 50: 73–78.

Willis, I. C., 1995: Intra-annual variations in glacier motion: a review. *Progress in Physical Geography*, 19(1): 61–106.

Willis, I., Arnold, N., and Brock, B., 2002: Effect of snowpack removal on energy balance, melt and runoff in a small supraglacial catchment. *Hydrological Processes*, 16: 2721–2749.

MS accepted June 2014